Multiplet effects on the $L_{2,3}$ fluorescence yield

of multiply ionized Ar*†

Mau Hsiung Chen and Bernd Crasemann

Department of Physics, University of Oregon

Eugene, Oregon 97403

The 2p fluorescence yield of Ar in the presence of 0 to 6 3p holes has been calculated by statistically averaging the fluorescence yields of initial states that consist of individual multiplet configurations, formed by coupling the 2p vacancy to the partially filled 3p shell. The $L_{2,3}$ fluorescence yield for the $(2p)^{-1}(3p)^{-n}$ configurations of Ar is found to be 1.48, 17.97, 22.62, 32.30, 78.79, 112.16, and 121.48×10^{-4} for n = 0, 1, 2, 3, 4, 5, and 6, respectively. Results agree reasonably well with experimental fluorescence yields deduced from ion-atom collision measurements.

*Research supported in part by the U. S. Army Research Office - Durham and by the National Aeronautics and Space Administration (Grant NGR 38-003-036).

†A preliminary report on this work was presented at the International Conference on X-Ray Processes in Matter, Otaniemi, Finland, 1974.

(NASA-CR-138836) MULTIPLET EFFECTS ON THE L(2,3) FLUORESCENCE YIELD OF MULTIPLY IONIZED Ar (Oregon Univ.) 30 p HC $4.50 CSCL 20H

N74-29152

Unclas

G3/24 42949

I. INTRODUCTION

We consider an atom that contains an inner-shell vacancy and a partially filled shell, other shells being full. The holes couple so that a multiplet structure results. The width of such multiplet states has recently been discussed by McGuire.[1] Radiationless transition probabilities to different multiplet states can vary substantially.[1,2]

In this paper, we report on calculations of the Ar 2p fluorescence yield in the presence of a partially filled 3p shell. The fluorescence yield $\omega(LS)$ is computed separately for each initial multiplet state of a given hole configuration $(2p)^{-1}(3p)^{-n}$, and $L_{2,3}$ fluorescence yields are calculated as weighted averages:

$$\bar{\omega}_{2,3} = \frac{\sum_{L,S} \omega(LS)\cdot(2L+1)(2S+1)}{\sum_{L,S} (2L+1)(2S+1)} \quad . \tag{1}$$

Because the various $\omega(LS)$ differ widely, the results differ considerably from $\bar{\omega}_{2,3}$ as calculated traditionally[3,4] from average Auger and radiative widths, each average extending over all multiplet states. It appears that the well-known discrepancy[5,6] between calculated and measured fluorescence yields of atoms with multiple inner-shell vacancies may, at least in some cases, be removed by the approach implicit in Eq. (1).

II. RADIATIONLESS TRANSITIONS

1. $(2p)^{-1}(3p)^{-n} \rightarrow (3p)^{-(n+2)}$ $[L_{2,3}-M_{2,3}M_{2,3}]$ transitions

McGuire[7] has derived general expressions, in LS coupling, for Auger rates in atoms with arbitrary vacancy structures, and has specialized them[1] for transitions of the type

$$(n_1\ell_1)[(n_3\ell_3)^n,\alpha_3L_3S_3]SL \rightarrow [(n_3\ell_3)^{n+2},\beta_3PQ].$$

The meaning of the subscripts to the quantum numbers is illustrated in Fig. 1; we have $n_3\ell_3 = n_4\ell_4$ in the class of transitions considered in this paragraph. The initial multiplet state, with quantum numbers SL, consists of n holes in the $n_3\ell_3$ shell, with quantum numbers $\alpha_3L_3S_3$, and one hole in the $n_1\ell_1$ shell. The final state consists of n+2 holes in the $n_3\ell_3$ shell, with quantum numbers β_3PQ. The radiationless transition probability is[8]

$$W_{fi}(LS,PQ) = (1/4)(n+1)(n+2)(2\ell_3+1) \prod_{i=1}^{3} (2\ell_i+1)(2P+1)(2Q+1)$$

$$\times \left| \sum_{f,g} (-1)^g[(2f+1)(2g+1)]^{1/2} I(KK'fg) \begin{Bmatrix} 1/2 & 1/2 & f \\ S_3 & Q & S \end{Bmatrix} \begin{Bmatrix} \ell_2 & \ell_1 & g \\ L_3 & P & L \end{Bmatrix} \right.$$

$$\left. \times (\ell_3^{\,n+2}\beta_3PQ\{| \ell_3^{\,2}fg;\ \ell_3^{\,n}\alpha_3L_3S_3) \right|^2 . \qquad (2)$$

The $\begin{Bmatrix} a & b & c \\ d & e & f \end{Bmatrix}$ are 6-j symbols. The two-electron coefficients of fractional parentage in Eq. (2) are defined as follows[1]:

$$(\ell^{n+2}\beta PQ\{| \ell^2 fg;\ell^n\alpha LS)$$

$$= -[(2f+1)(2g+1)]^{1/2} \sum_{\gamma P'Q'} [(2P'+1)(2Q'+1)]^{1/2} \begin{Bmatrix} L & \ell & P' \\ \ell & P & g \end{Bmatrix}$$

$$\times \begin{Bmatrix} S & 1/2 & Q' \\ 1/2 & Q & f \end{Bmatrix} (\ell^{n+2}\beta PQ\{|\ell^{n+1}\gamma P'Q') \times (\ell^{n+1}\gamma P'Q'\{|\ell^{n}\alpha LS), \qquad (3)$$

where the $(\ell^m\beta PQ\{|\ell^{m-1}\gamma P'Q')$ are the usual coefficients of fractional parentage.

We have

$$I(KK'fg) = \sum_K D(K) \begin{Bmatrix} \ell_1 & \ell_3 & K \\ \ell_4 & \ell_2 & g \end{Bmatrix} + (-1)^{f-g} \sum_{K'} E(K') \begin{Bmatrix} \ell_1 & \ell_4 & K' \\ \ell_3 & \ell_2 & g \end{Bmatrix}. \qquad (4)$$

The terms containing the direct and exchange matrix elements are

$$D(K) = R_K(\ell_1\ell_2\ell_3\ell_4) \begin{pmatrix} \ell_1 & K & \ell_3 \\ 0 & 0 & 0 \end{pmatrix} \begin{pmatrix} \ell_2 & K & \ell_4 \\ 0 & 0 & 0 \end{pmatrix}, \qquad (5)$$

$$E(K) = R_K(\ell_1\ell_2\ell_4\ell_3) \begin{pmatrix} \ell_1 & K & \ell_4 \\ 0 & 0 & 0 \end{pmatrix} \begin{pmatrix} \ell_2 & K & \ell_3 \\ 0 & 0 & 0 \end{pmatrix}, \qquad (6)$$

where the $\begin{pmatrix} a & b & c \\ 0 & 0 & 0 \end{pmatrix}$ are 3-j symbols. The radial integrals R_K are defined in Sec. III.

2. $(2p)^{-1}(3p)^{-n} \rightarrow (3s)^{-1}(3p)^{-(n+1)}$ $[L_{2,3}-M_1M_{2,3}]$ transitions

The Auger rate for transitions of the type

$(n_1\ell_1)[(n_4\ell_4)^p, S_4L_4]SL \rightarrow (n_3\ell_3)[(n_4\ell_4)^{p+1}, Q_4P_4]QP$ is[1,8]

$$W_{fi}(LS,PQ) = (2P+1)(2Q+1) \prod_{i=1}^{4} (2\ell_i+1)(p+1) \sum_{P_4Q_4} (2P_4+1)(2Q_4+1)$$

$$\times (\ell_4^{p+1}\beta_4 P_4 Q_4 \{| \ell_4^{p}\alpha_4 L_4 S_4)^2 \times \left| \sum_{f,g} (-1)^f I(KK'fg)(2f+1)(2g+1) \right.$$

$$\times \left. \begin{Bmatrix} P & g & L_4 \\ \ell_1 & L & \ell_2 \end{Bmatrix} \begin{Bmatrix} g & \ell_4 & \ell_3 \\ P_4 & P & L_4 \end{Bmatrix} \begin{Bmatrix} Q & f & S_4 \\ 1/2 & S & 1/2 \end{Bmatrix} \begin{Bmatrix} f & 1/2 & 1/2 \\ Q_4 & Q & S_4 \end{Bmatrix} \right|^2 \qquad (7)$$

where the subscripts to the quantum numbers denote shells identified in Fig. 1.

3. $(2p)^{-1}(3p)^{-n} \rightarrow (3s)^{-2}(3p)^{-n}$ $[L_{2,3}-M_1M_1]$ transitions

For this class of transitions, which accounts for only ~2% of the 2p Auger width, we neglect the effect of the partially filled 3p shell and compute the Auger rate in the traditional manner.[9]

III. RADIATIONLESS TRANSITION PROBABILITIES IN TERMS OF RADIAL MATRIX ELEMENTS

The Auger transition probabilities for each initial multiplet state were calculated, in terms of radial matrix elements, with the aid of a computer program that includes 3-j and 6-j symbol subroutines.

The radial integrals are

$$R_K(n_1\ell_1,n_2\ell_2,n_3\ell_3,n_4\ell_4) \equiv R_K(\ell_1\ell_2\ell_3\ell_4)$$

$$= \int_{r_1,r_2=0}^{\infty} r_1^2 r_2^2 \gamma_K R_{n_1\ell_1}(r_1) R_{n_2\ell_2}(r_2) R_{n_3\ell_3}(r_1) R_{n_4\ell_4}(r_2)\, dr_1 dr_2, \qquad (8)$$

where

$$\gamma_K = \begin{cases} r_1^K/r_2^{K+1}, & r_1 < r_2 \\ r_2^K/r_1^{K+1}, & r_1 > r_2 \end{cases} \qquad (9)$$

and the subscripts 1....4 pertain to the states identified in Fig. 1.

Results for atoms with one to 5 holes in the 3p shell are listed in Tables I-V. For the case on an empty 3p level (6 holes), the familiar closed-shell results apply.[10]

IV. SUM RULES

For $(2p)^{-1}(3p)^{-n} \rightarrow (3p)^{-(n+2)}$ transitions, we find

$$\overline{W}_{fi} = \frac{\sum_{L_3,S_3} \sum_{P,Q} \sum_{L,S} (2L+1)(2S+1) W_{fi}\big((L_3S_3)LS,PQ\big)}{(4\ell_1+2)\left[\sum_{L_3S_3} (2L_3+1)(2S_3+1)\right]}$$

$$= \frac{(4\ell_3+2-n)(4\ell_3+1-n)}{(4\ell_3+2)(4\ell_3+1)} I_0 , \qquad (10)$$

where

$$I_0 = 1/2 \; \frac{(2\ell_3+1)\prod_{i=1}^{3}(2\ell_i+1)}{4\ell_1+2} \sum_{f,g} (2f+1)(2g+1) I(KK'fg)^2 \qquad (11)$$

is the full-shell rate.

The corresponding sum rule for $(2p)^{-1}(3p)^{-n} \rightarrow (3s)^{-1}(3p)^{-(n+1)}$ transitions has been derived by McGuire[1]:

$$\sum_{\substack{L,S \\ P_4,Q_4 \\ P,Q}} W_{fi}(LS,PQ) = \prod_{i=1}^{4} \frac{(2\ell_i+1)(4\ell_4+2-p)}{(4\ell_1+2)(4\ell_4+2)}$$

$$\times \sum_{f,g} (2f+1)(2g+1)I(KK'fg)^2 = \frac{4\ell_4+2-p}{4\ell_4+2} I_0, \qquad (12)$$

where the full-shell rate is

$$I_0 = \prod_{i=1}^{4} \frac{(2\ell_i+1)}{4\ell_1+2} \sum_{f,g} (2f+1)(2g+1)I(KK'fg)^2 . \qquad (13)$$

Equations (10) and (12) were used to check both algebraic and numerical results of the present work.

V. TRANSITION RATES AND FLUORESCENCE YIELDS

Radial matrix elements were calculated from Hartree-Fock-Slater one-electron radial eigenfunctions with Xα exchange. The wave functions were generated using the appropriate potential for each individual defect configuration. The frozen-orbitals approximation was used, assuming that the initial and final one-electron wave functions are the same.

X-ray and Auger energies for the various configurations were taken from the work of Larkins,[11] who used the Hartree-Fock approach to calculate the total energy difference in adiabatic approximation.

The radiative transition rates, in dipole approximation, are the same for the various multiplet states of each initial hole configuration, if multiplet energy splitting (approximately 2 eV out of 240 eV) is neglected (Table VI).

Auger rates to the 2p hole and $L_{2,3}$ fluorescence yields for the various initial multiplet states are summarized in Table VII. Average fluorescence yields for each hole configuration, computed according to Eq. (1), are listed in Table VIII.

VI. COMPARISON WITH EXPERIMENT

These calculations were performed for the specific case of the Ar 2p fluorescence yield in the presence of 3p vacancies because Fortner[6,12] has recently made a comprehensive set of measurements on this system. L x rays emitted in Ar+Ar collisions at various energies were analyzed with a Bragg spectrometer, and the unfolded peaks were correlated with various vacancy states on the basis of adiabatic Hartree-Fock calculations of energy shifts.[6] Fortner noted that in most cases > 90% of the observed x rays were from 3s → 2p transitions in atoms with a single L vacancy. Fortner derived experimental fluorescence yields by dividing the measured x-ray production cross sections by total L-shell ionization cross sections $\sigma_I = 2\pi r_x^2$, where r_x is the level-crossing radius. The measured fluorescence yields can be compared with theoretical results through the relation

$$(\bar{\omega})^{-1} = \Sigma(N_i/\omega_i), \tag{14}$$

where N_i is the fractional X-ray yield corresponding to vacancy configuration i with fluorescence yield ω_i.

Uncertainties in the analysis arise from the deconvolution of the x-ray spectra, from the fact that 3s and 3p vacancies could not be distinguished with the available spectrometer resolution, and from some degeneracy between transitions to double and single L vacancies. Fortner showed that Eq. (14), with traditionally computed theoretical fluorescence yields for various M-shell defect configurations,[3,4,13] leads to results that fall below measured fluorescence yields by a factor of ~4.4 (Fig. 2).

The present calculation leads to considerably better agreement with experiment, as illustrated in Fig. 2. Here we have taken Fortner's analysis[6] of L x rays from Ar^++Ar collisions at various energies and computed effective fluorescence yields with the theoretical results of Table VIII. For projectile energies below 130 keV, we assumed that only single 2p vacancies were created in the collisions, because at these energies Fortner's spectra[6] do not show the signature of double L-hole events, viz., (1) x rays shifted ~25 eV up from transitions to a single L vacancy in the presence of n 3p holes, and (2) x rays that correspond to a single L vacancy in the presence of n+2 3p holes. At bombarding energies of 130 keV and above, there is evidence for the production of double L vacancies, and we have multiplied the calculated effective fluorescence yields by a factor of 1.4 to account for this effect, as suggested by Fortner.[6]

Except at 40 keV, calculated and measured fluorescence yields agree to better than 30%. The calculated yield at 40 keV would agree much better with experiment if the number of L x rays emitted by Ar atoms without any 3p vacancies were somewhat smaller than the 9% indicated by Fortner's analysis.

The results of the present calculations can also be tested by comparison with the measured effective L fluorescence yield[6] in 90-keV $Ar^{+}\rightarrow CH_4$ collisions, which is $19X10^{-4}$. Using Fortner's analysis which indicates that 68% of the x rays originate from Ar atoms with one 3p vacancy and 20% from Ar atoms with two 3p vacancies, and not including the 12% of unidentified x rays above 253 eV, we find from Table VIII a calculated value of $\omega_L=21.42x10^{-4}$.

The discrepancies that remain may, at least in part, be due to the experimental uncertainties discussed above and to the fact that the various initial multiplet states may not always be populated statistically in collision events.[14]

ACKNOWLEDGMENTS

We are much indebted to Dr. E. J. McGuire of the Sandia Laboratories and Dr. R. J. Fortner of the Lawrence Livermore Laboratory for communicating their results to us in advance of publication. It is a pleasure to acknowledge helpful conversations with Dr. D. A. Ringers.

References

[1]E. J. McGuire, Phys. Rev. A 10, xxx (1974).

[2]C. P. Bhalla, Phys. Lett. 46A, 185 (1973).

[3]F. P. Larkins, J. Phys. B 4, L29 (1971).

[4]C. P. Bhalla and D. L. Walters, in Proc. Intl. Conf. Inner-Shell Ionization Phenomena, ed. by R. W. Fink, S. T. Manson, J. M. Palms, and P. Venugopala Rao, U. S. Atomic Energy Commission Report No. CONF-720404 (1973), p. 1572.

[5]V. R. Veluri, F. E. Wood, J. M. Palms, and P. Venugopala Rao, in Proc. Intl. Conf. Inner-Shell Ionization Phenomena, ed. by R. W. Fink, S. T. Manson, J. M. Palms, and P. Venugopala Rao, U. S. Atomic Energy Commission Report No. CONF-720404 (1973), p. 251.

[6]R. J. Fortner, Phys. Rev. A (to be published).

[7]E. J. McGuire, in Atomic Inner-Shell Processes, ed. by B. Crasemann (Academic Press, in press).

[8]This expression differs by $(2\pi)^{-1}$ from the result given in Ref. 1, because our normalization of the continuum state differs from McGuire's by 2π.

[9]M. H. Chen, B. Crasemann, and V. O. Kostroun, Phys. Rev. A 4, 1 (1971).

[10]R. A. Rubenstein, thesis, University of Illinois, 1955 (unpublished).

[11]F. P. Larkins, J. Phys. B 4, 1 (1971).

[12]R. J. Fortner, Bull. Am. Phys. Soc. 18, 1575 (1973).

[13]C. P. Bhalla, in Proceedings of the 5th International Conference on Atomic Collisions in Solids, Gatlinburg, Tennessee, September 1973 (to be published).

[14]C. P. Bhalla, D. L. Matthews, and C. F. Moore, Phys. Lett. 46A, 336 (1974).

TABLE I. Auger transition probabilities to an initial 2p vacancy in an atom with the electron configuration $(1s)^2(2s)^2(2p)^5(3s)^2(3p)^5$, for various initial multiplet states. Results are given in terms of radial integrals $R_K(\ell_1\ell_2\ell_3\ell_4)$ as defined in Eq. (8).

Multiplet state	Auger transition probability
^1S	$(1/9)R_1(1100)^2 + 8R_0(1111)^2 - (16/5)R_0(1111)R_2(1111) + (8/25)R_2(1111)^2 + (1/9)R_1(1001)^2 - (4/3)R_1(1001)R_0(1010) + 4R_0(1010)^2 + (2/9)R_1(1201)^2 - (8/15)R_1(1201)R_2(1210) + (8/25)R_2(1210)^2$
^1P	$(1/9)R_1(1100)^2 + (36/125)R_2(1111)^2 + (9/125)R_2(1311)^2 + (1/3)R_1(1001)^2 + (1/3)R_1(1201)^2 - (2/5)R_1(1201)R_2(1210) + (6/25)R_2(1210)^2$
^1D	$(1/9)R_1(1100)^2 + 8R_0(1111)^2 - (44/25)R_0(1111)R_2(1111) + (74/625)R_2(1111)^2 + (81/625)R_2(1311)^2 + (19/45)R_1(1201)^2 - (22/75)R_1(1210)R_2(1210) + (22/125)R_2(1210)^2 + (1/9)R_1(1001)^2 - (4/3)R_1(1001)R_0(1010) + 4R_0(1010)^2$
^3S	$(1/9)R_1(1100)^2 + (1/9)R_1(1001)^2 + (2/9)R_1(1201)^2$
^3P	$(1/9)R_1(1100)^2 + 8R_0(1111)^2 - (4/5)R_0(1111)R_2(1111) + (16/125)R_2(1111)^2 + (9/125)R_2(1311)^2 + (1/3)R_1(1001)^2 - (4/3)R_1(1001)R_0(1010) + 4\ R_0(1010)^2 + (1/3)R_1(1201)^2 - (2/15)R_1(1201)R_2(1210) + (2/25)R_2(1210)^2$

TABLE I. (Continued)

Multiplet state	Auger transition probability
^3D	$(1/9)R_1(1100)^2 + (54/625)R_2(1111)^2 + (81/625)R_2(1311)^2 + (1/9)R_1(1001)^2 + (19/45)R_1(1201)^2 - (6/25)R_1(1201)R_2(1210) + (18/125)R_2(1210)^2$

TABLE II. Auger transition probabilities to an initial 2p vacancy in an atom with the electron configuration $(1s)^2(2s)^2(2p)^5(3s)^2(3p)^4$, for various initial multiplet states. Results are given in terms of radial integrals $R_K(\ell_1\ell_2\ell_3\ell_4)$ as defined in Eq. (8).

Multiplet state	Auger transition probability
$(^1S)^2P$	$(1/9)R_1(1100)^2 + 2R_0(1111)^2 + (14/125)R_2(1111)^2 + (6/125)R_2(1311)^2 + (4/3)R_0(1010)^2 - (4/9)R_0(1010)R_1(1001) + (4/27)R_1(1001)^2 + (8/27)R_1(1201)^2 - (8/45)R_1(1201)R_2(1210) + (8/75)R_2(1210)^2$
$(^3P)^2S$	$(1/9)R_1(1100)^2 + (9/25)R_2(1111)^2 + (4/9)R_1(1001)^2 + (2/9)R_1(1201)^2 - (2/5)R_1(1201)R_2(1210) + (6/25)R_2(1210)^2$
$(^3P)^2P$	$(1/9)R_1(1100)^2 + (9/2)R_0(1111)^2 - (9/5)R_0(1111)R_2(1111) + (9/50)R_2(1111)^2 + 3R_0(1010)^2 - R_0(1010)R_1(1001) + (1/9)R_1(1001)^2 + (2/9)R_1(1201)^2 - (2/5)R_1(1201)R_2(1210) + (6/25)R_2(1210)^2$
$(^3P)^2D$	$(1/9)R_1(1100)^2 + (9/2)R_0(1111)^2 - (27/25)R_0(1111)R_2(1111) + (117/1250)R_2(1111)^2 + (54/625)R_2(1311)^2 + 3R_0(1010)^2 - R_0(1010)R_1(1001) + (1/9)R_1(1001)^2 + (16/45)R_1(1201)^2 - (8/25)R_1(1201)R_2(1210) + (24/125)R_2(1210)^2$
$(^3P)^4S$	$(1/9)R_1(1100)^2 + 9R_0(1111)^2 + (4/9)R_1(1001)^2 - 2R_1(1001)R_0(1010) + 6R_0(1010)^2 + (2/9)R_1(1201)^2$

TABLE II. (Continued)

Multiplet state	Auger transition probability
$(^3P)\,^4P$	$(1/9)R_1(1100)^2 + (1/9)R_1(1001)^2 + (2/9)R_1(1201)^2$
$(^3P)\,^4D$	$(1/9)R_1(1100)^2 + (36/625)R_2(1111)^2$
	$+ (54/625)R_2(1311)^2 + (16/45)R_1(1201)^2$
	$- (4/25)R_1(1201)R_2(1210) + (12/125)R_2(1210)^2 + (1/9)R_1(1001)$
$(^1D)\,^2P$	$(1/9)R_1(1100)^2 + (5/2)R_0(1111)^2 - (3/5)R_0(1111)R_2(1111)$
	$+ (73/1250)R_2(1111)^2 + (6/625)R_2(1311)^2 + (5/3)R_0(1010)^2$
	$- (5/9)R_1(1001)R_0(1010) + (5/27)R_1(1001)^2$
	$+ (14/135)R_1(1201)^2 - (14/225)R_1(1201)R_2(1210)$
	$+ (14/375)R_2(1210)^2$
$(^1D)\,^2D$	$(1/9)R_1(1100)^2 + (9/2)R_0(1111)^2 - (9/25)R_0(1111)R_2(1111)$
	$+ (153/1250)R_2(1111)^2 + (36/625)R_2(1311)^2$
	$+ (4/15)R_1(1201)^2 - (4/25)R_1(1201)R_2(1210)$
	$+ (12/125)R_2(1210)^2 + (1/3)R_1(1001)^2$
	$- R_1(1001)R_0(1010) + 3R_0(1010)^2$
$(^1D)\,^2F$	$(1/9)R_1(1100)^2 + (9/625)R_2(1111)^2$
	$+ (522/4375)R_2(1311)^2 + (2/5)R_1(1201)^2$
	$- (6/25)R_1(1201)R_2(1210) + (18/125)R_2(1210)^2$

TABLE III. Auger transition probabilities to an initial 2p vacancy in an atom with the electron configuration $(1s)^2(2s)^2(2p)^5(3s)^2(3p)^3$, for various initial multiplet states. Results are given in terms of radial integrals $R_K(\ell_1\ell_2\ell_3\ell_4)$ as defined in Eq. (8).

Multiplet state	Auger transition probability
$(^4S)^3P$	$(1/9)R_1(1100)^2 + (8/3)[R_0(1111) - (1/5)R_2(1111)]^2$
	$+ (1/9)R_1(1001)^2 - (8/9)R_1(1001)R_0(1010)$
	$+ (8/3)R_0(1010)^2 + (2/9)R_1(1201)^2$
	$- (16/45)R_1(1201)R_2(1210) + (16/75)R_2(1210)^2$
$(^4S)^5P$	$(1/9)R_1(1100)^2 + (1/9)R_1(1001)^2 + (2/9)R_1(1201)^2$
$(^2P)^1S$	$(1/9)R_1(1100)^2 + 8[R_0(1111) - (1/5)R_2(1111)]^2$
	$+ (2/9)R_1(1001)^2 - (8/3)R_1(1001)R_0(1010)$
	$+ 8R_0(1010)^2 + (1/9)R_1(1201)^2 - (4/15)R_1(1201)R_2(1210)$
	$+ (4/25)R_2(1210)^2$
$(^2P)^1P$	$(1/9)R_1(1100)^2 + (9/50)R_2(1111)^2 + (1/6)R_1(1001)^2$
	$+ (1/6)R_1(1201)^2 - (1/5)R_1(1201)R_2(1210)$
	$+ (3/25)R_2(1210)^2$
$(^2P)^1D$	$(1/9)R_1(1100)^2 + 2[R_0(1111) - (1/50)R_2(1111)]^2$
	$+ (27/625)R_2(1311)^2 + (1/18)R_1(1001)^2$
	$- (2/3)R_1(1001)R_0(1010) + 2R_0(1010)^2$
	$+ (5/18)R_1(1201)^2 - (23/75)R_1(1201)R_2(1210) + (23/125)R_2(1210)$
$(^2P)^3S$	$(1/9)R_1(1100)^2 + (2/9)R_1(1001)^2 + (1/9)R_1(1201)^2$

TABLE III. (Continued)

Multiplet state	Auger transition probability
$(^2P)^3P$	$(1/9)R_1(1100)^2 + (1/2)[2R_0(1111) + (1/5)R_2(1111)]^2$
	$+ (1/6)R_1(1001)^2 - (2/3)R_1(1001)R_0(1010)$
	$+ 2R_0(1010)^2 + (1/6)R_1(1201)^2 - (1/15)R_1(1201)R_2(1210)$
	$+ (1/25)R_2(1210)^2$
$(^2P)^3D$	$(1/9)R_1(1100)^2 + (81/1250)R_2(1111)^2 + (27/625)R_2(1311)^2$
	$+ (5/18)R_1(1201)^2 - (3/25)R_1(1201)R_2(1210)$
	$+ (9/125)R_2(1210)^2 + (1/18)R_1(1001)^2$
$(^2D)^1P$	$(1/9)R_1(1100)^2 + (27/250)R_2(1111)^2 + (1/18)R_1(1201)$
	$+ (9/125)R_2(1210)^2 + (5/18)R_1(1001)^2 - (3/25)R_1(1201)R_2(1210)$
$(^2D)^1D$	$(1/9)R_1(1100)^2 + (3/2)[2R_0(1111) - (7/25)R_2(1111)]^2$
	$+ (9/625)R_2(1311)^2 + (1.6)R_1(1201)^2$
	$- (7/25)R_1(1201)R_2(1210) + (21/125)R_2(1210)^2$
	$+ (1/6)R_1(1001)^2 - 2R_1(1001)R_0(1010) + 6R_0(1010)^2$
$(^2D)^1F$	$(1/9)R_1(1100)^2 + (72/875)R_2(1311)^2$
	$+ (1/3)R_1(1201)^2 - (8/25)R_1(1201)R_2(1210)$
	$+ (24/125)R_2(1210)^2$
$(^2D)^3P$	$(1/9)R_1(1100)^2 + (5/6)[-2R_0(1111) + (1/25)R_2(1111)]^2$
	$+ (5/18)R_1(1001)^2 - (10/9)R_1(1001)R_0(1010)$
	$+ (10/3)R_0(1010)^2 + (1/90)R_1(1201)^2$
	$- (1/225)R_1(1201)R_2(1210) + (1/375)R_2(1210)^2$

TABLE III. (Continued)

Multiplet state	Auger transition probability
$(^2D)^3D$	$(1/9)R_1(1100)^2 + (27/1250)R_2(1111)^2 + (9/625)R_2(1311)^2$ $+ (1/6)R_1(1201)^2 - (1/25)R_1(1201)R_2(1210)$ $+ (3/125)R_2(1210)^2 + (1/6)R_1(1001)^2$
$(^2D)^3F$	$(1/9)R_1(1100)^2 + (72/875)R_2(1311)^2 + (1/3)R_1(1201)^2$ $- (4/25)R_1(1201)R_2(1210) + (12/125)R_2(1210)^2$

TABLE IV. Auger transition probabilities to an initial 2p vacancy in an atom with the electron configuration $(1s)^2(2s)^2(2p)^5(3s)^2(3p)^2$, for various initial multiplet states. Results are given in terms of radial integrals $R_K(\ell_1\ell_2\ell_3\ell_4)$ as defined in Eq. (8).

Multiplet state	Auger transition probability
$(^1S)^2P$	$(1/9)R_1(1100)^2 + (1/3)[R_0(1111) + (2/5)R_2(1111)]^2$ $+ (4/54)R_1(1001)^2 - (2/9)R_1(1001)R_0(1010)$ $+ (2/3)R_0(1010)^2 + (4/27)R_1(1201)^2 - (4/45)R_1(1201)R_2(1210)$ $+ (4/75)R_2(1210)^2$
$(^3P)^2S$	$(1/9)R_1(1100)^2$
$(^3P)^2P$	$(1/9)R_1(1100)^2 + 3[-R_0(1111) + (1/5)R_2(1111)]^2$ $+ (2/9)R_1(1001)^2 - 2R_1(1001)R_0(1010) + 6R_0(1010)^2$ $+ (1/9)R_1(1201)^2 - (1/5)R_1(1201)R_2(1210)$ $+ (3/25)R_2(1210)^2$
$(^3P)^2D$	$(1/9)R_1(1100)^2 + (1/5)R_1(1201)^2 - (9/25)R_1(1201)R_2(1210)$ $+ (27/125)R_2(1210)^2$
$(^3P)^4S$	$(1/9)R_1(1100)^2$
$(^3P)^4P$	$(1/9)R_1(1100)^2 + (2/9)R_1(1001)^2 + (1/9)R_1(1201)^2$
$(^3P)^4D$	$(1/9)R_1(1100)^2 + (1/5)R_1(1201)^2$
$(^1D)^2P$	$(1/9)R_1(1100)^2 + (5/3)[R_0(1111) + (1/25)R_2(1111)]^2$ $+ (10/27)R_1(1001)^2 - (10/9)R_1(1001)R_0(1010)$ $+ (10/3)R_0(1010)^2 + (1/135)R_1(1201)^2$ $- (1/225)R_1(1201)R_2(1210) + (1/375)R_2(1210)^2$

TABLE IV. (Continued)

Multiplet state	Auger transition probability
$(^1D)^2D$	$(1/9)R_1(1100)^2 + (1/15)R_1(1201)^2$ $- (1/25)R_1(1201)R_2(1210) + (3/125)R_2(1210)^2$
$(^1D)^2F$	$(1/9)R_1(1100)^2 + (54/875)R_2(1311)^2$ $+ (4/15)R_1(1201)^2 - (4/25)R_1(1201)R_2(1210)$ $+ (12/125)R_2(1210)^2$

TABLE V. Auger transition probabilities to an initial 2p vacancy in an atom with the electron configuration $(1s)^2(2s)^2(2p)^5(3s)^2(3p)$, for various initial multiplet states. Results are given in terms of radial integrals $R_K(\ell_1\ell_2\ell_3\ell_4)$ as defined in Eq. (8).

Multiplet state	Auger transition probability
^1S	$(1/9)R_1(1100)^2 + 3[-(1/3)R_1(1001) + 2R_0(1010)]^2$
^1P	$(1/9)R_1(1100)^2$
^1D	$(1/9)R_1(1100)^2 + (6/5)[(1/3)R_1(1201) - (2/5)R_2(1210)]^2$
^3S	$(1/9)R_1(1100)^2 + (1/3)R_1(1001)^2$
^3P	$(1/9)R_1(1100)^2$
^3D	$(1/9)R_1(1100)^2 + (2/15)R_1(1201)^2$

TABLE VI. Argon 2p radiative widths (in multiples of 10^{-7} a.u.) for various initial hole configurations.

Initial configuration	Radiative width
$(2p)^{-1}$	8.633
$(2p)^{-1}(3p)^{-1}$	8.788
$(2p)^{-1}(3p)^{-2}$	9.558
$(2p)^{-1}(3p)^{-3}$	10.425
$(2p)^{-1}(3p)^{-4}$	11.389
$(2p)^{-1}(3p)^{-5}$	12.46
$(2p)^{-1}(3p)^{-6}$	13.24

TABLE VII. Radiationless transition probabilities (in multiples of 10^{-3} a.u.) and fluorescence yields (in multiples of 10^{-4}) for an Ar 2p vacancy in the presence of a partially filled 3p shell, for given initial multiplet states.

Initial hole configuration	Initial multiplet term	Auger rate	Fluorescence yield
$(2p)^{-1}(3p)^{-1}$	^1S	9.210	0.954
	^1P	0.479	18.34
	^1D	10.235	0.859
	^3S	0.133	66.15
	^3P	10.906	0.806
	^3D	0.347	25.31
$(2p)^{-1}(3p)^{-2}$	$(^1S)^2P$	3.743	2.553
	$(^3P)^2S$	0.544	17.566
	$(^3P)^2P$	6.616	1.445
	$(^3P)^2D$	7.254	1.318
	$(^3P)^4S$	15.859	0.603
	$(^3P)^4P$	0.150	63.635
	$(^3P)^4D$	0.285	33.56
	$(^1D)^2P$	4.090	2.337
	$(^1D)^2D$	7.917	1.207
	$(^1D)^2F$	0.2676	35.717

TABLE VII. (Continued)

Initial hole configuration	Initial multiplet term	Auger rate	Fluorescence yield
$(2p)^{-1}(3p)^{-3}$	$(^4S)^3P$	5.277	1.976
	$(^4S)^5P$	0.169	61.686
	$(^2P)^1S$	15.580	0.669
	$(^2P)^1P$	0.309	33.738
	$(^2P)^1D$	4.620	2.256
	$(^2P)^3S$	0.254	41.043
	$(^2P)^3P$	5.060	2.060
	$(^2P)^3D$	0.236	44.174
	$(^2D)^1P$	0.354	29.449
	$(^2D)^1D$	12.295	0.848
	$(^2D)^1F$	0.228	45.724
	$(^2D)^3P$	7.660	1.361
	$(^2D)^3D$	0.248	42.036
	$(^2D)^3F$	0.228	45.724
$(2p)^{-1}(3p)^{-4}$	$(^1S)^2P$	1.592	18.13
	$(^3P)^2S$	0.0909	125.28
	$(^3P)^2P$	9.411	1.210
	$(^3P)^2D$	0.0912	124.88
	$(^3P)^4S$	0.0909	125.28
	$(^3P)^4P$	0.281	40.52
	$(^3P)^4D$	0.0920	123.79
	$(^1D)^2P$	6.234	1.827
	$(^1D)^2D$	0.0912	124.88
	$(^1D)^2F$	0.212	53.80

TABLE VII. (Continued)

Initial hole configuration	Initial multiplet term	Auger rate	Fluorescence yield
$(2p)^{-1}(3p)^{-5}$	^1S	12.25	1.017
	^1P	0.0994	123.81
	^1D	0.0995	123.68
	^3S	0.412	30.14
	^3P	0.0994	123.81
	^3D	0.1002	122.82
$(2p)^{-1}(3p)^{-6}$	^2P	0.1093	121.48

TABLE VIII. Argon average $L_{2,3}$ fluorescence yields (in multiples of 10^{-4}) for various $(2p)^{-1}(3p)^{-n}$ configurations.

Initial hole configuration	2p fluorescence yield
$(2p)^{-1}$	1.48
$(2p)^{-1}(3p)^{-1}$	17.97
$(2p)^{-1}(3p)^{-2}$	22.62
$(2p)^{-1}(3p)^{-3}$	32.30
$(2p)^{-1}(3p)^{-4}$	78.79
$(2p)^{-1}(3p)^{-5}$	112.16
$(2p)^{-1}(3p)^{-6}$	121.48

Figure Captions

FIG. 1. Schematic representation of a radiationless transition, indicating designation of states. (In the exchange transition, the roles of $n_3\ell_3$ and $n_4\ell_4$ are interchanged.)

FIG. 2. Measured effective argon L fluorescence yields, $\bar{\omega}_L = \sigma_x/\sigma_I$, as a function of bombarding energy, after Ref. 6. Calculated yields based on Refs. 3,4, and 13 fall near the dashed curve, which represents the measurements divided by 4.4 (Ref. 6). The crosses indicate calculations from yields for individual initial-state multiplet configurations (Table VIII).

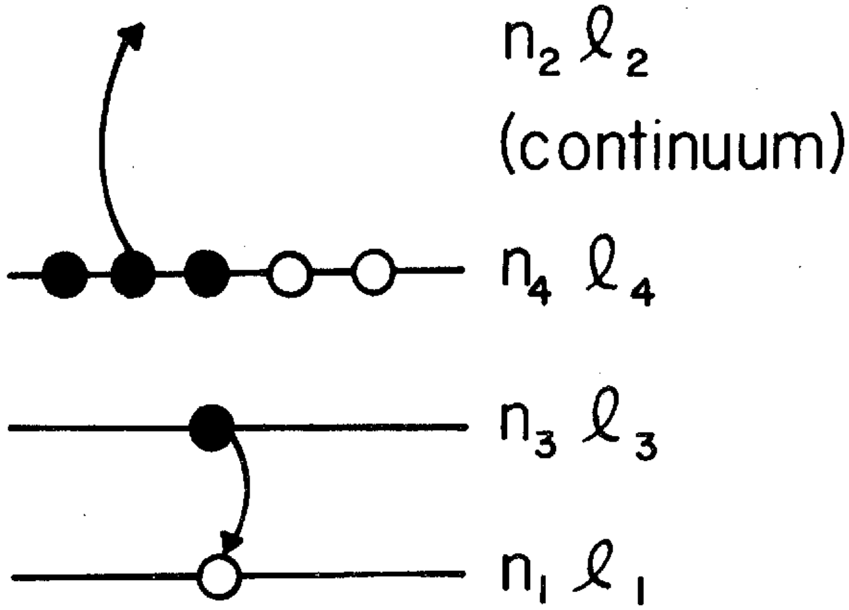
$n_2 \ell_2$
(continuum)
$n_4 \ell_4$
$n_3 \ell_3$
$n_1 \ell_1$

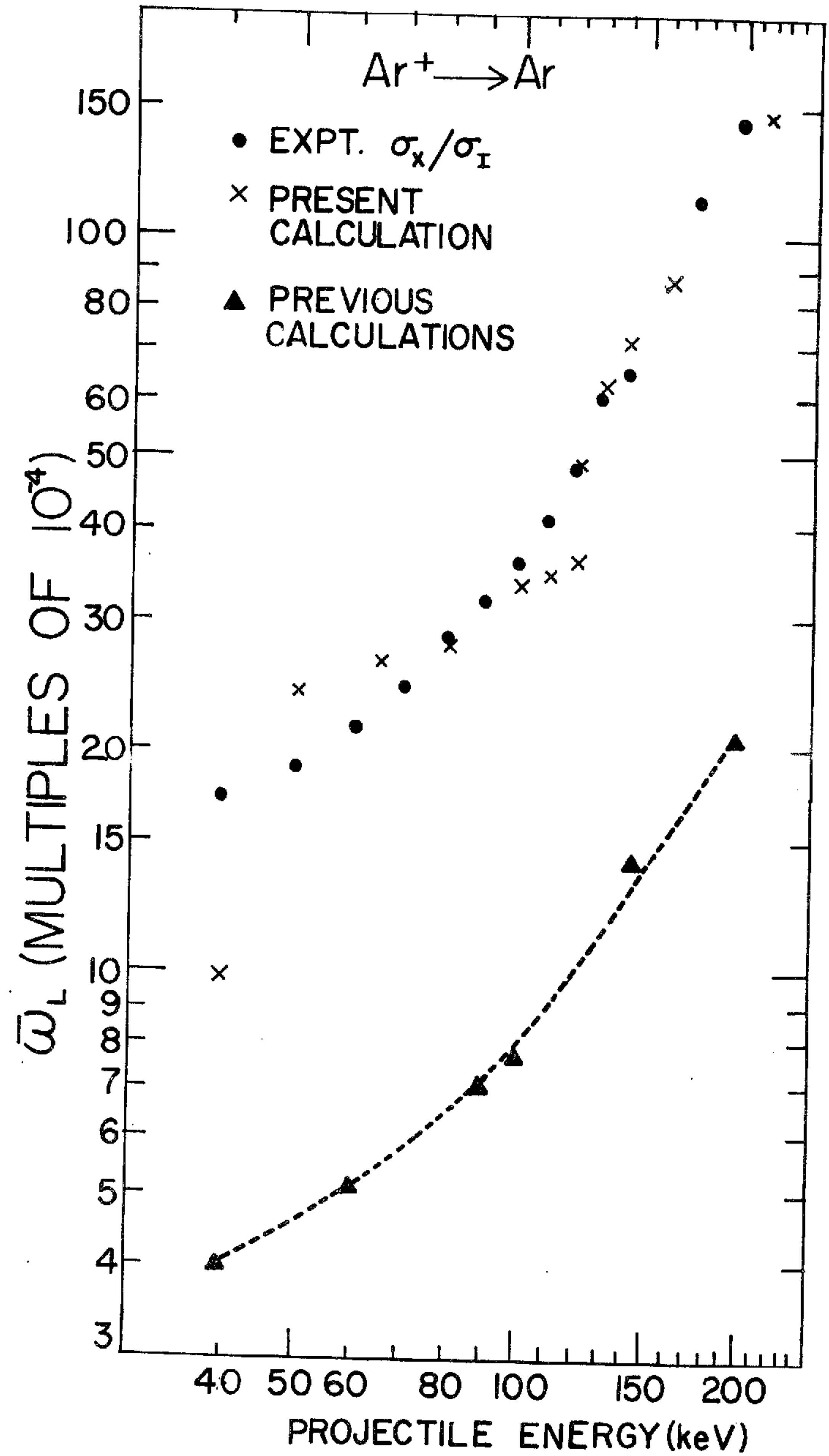
Ar⁺ → Ar
EXPT. σ_x/σ_I
PRESENT CALCULATION
PREVIOUS CALCULATIONS
$\bar{\omega}_L$ (MULTIPLES OF 10^4)
150
100
80
60
50
40
30
20
15
10
9
8
7
6
5
4
3
40
50
60
80
100
150
200
PROJECTILE ENERGY (keV)